Acta Cryst. (1996). B52, 842–853

Trimorphism of 2,2′-Dipyridylamine: Structures, Phase Transitions and Thermodynamic Stabilities

HOLGER SCHÖDEL, CHRISTIAN NÄTHER, HANS BOCK* AND FRAUKE BUTENSCHÖN

Department of Chemistry, Johann Wolfgang Goethe University, Marie-Curie-Strasse 11, D-60439 Frankfurt/Main, Germany. E-mail: schoedel@bock.anorg.chemie.uni-frankfurt.de

(Received 27 February 1996; accepted 3 April 1996)

Abstract

Crystals of an unknown third crystalline modification of 2,2′-dipyridylamine were obtained from acetone solution and their crystal structure was determined at both 150 K and room temperature. In contrast to the known orthorhombic and triclinic forms, which contain hydrogen-bridged dimers, the molecules of the monoclinic polymorph are arranged in tetramers. The crystallographic results for the monoclinic form are presented here, as well as a detailed comparison of crystal and molecular structures of the three polymorphs. Studies by differential thermal analysis (DTA) and optical microscopy, performed with single crystals, show a transformation of the orthorhombic phase at ~323 K and of the monoclinic form at ~368 K. According to powder diffraction studies, transformation of the low melting orthorhombic polymorph results in a mixture of monoclinic and triclinic phases, whereas the monoclinic modification transforms into the triclinic phase just below its melting point at 368 K. The single crystals of both forms are destroyed during the conversion and, therefore, in both cases a reconstructive transition *via* nucleation and growth should occur. The conditions for the crystallization of the distinct modifications and their relative thermodynamic stabilities are investigated in different solvents and at different temperatures. Independent of the solvent chosen, the orthorhombic form is the most stable below 263 K. In the range between 263 and 313 K the monoclinic form appears to be thermodynamically advantageous and above that temperature, the stability order is changed in favour of the triclinic polymorph. Based on the experimental results, a qualitative free energy–temperature diagram is provided.

1. Introduction

2,2′-Dipyridylamine, first prepared in 1914 from 2-chloro- and 2-aminopyridine (Tschitschibabin & Zeide, 1914), is of considerable interest as a ligand for alkaline earth as well as transition metal complexes and mainly for the copper(II) ion. The effective stabilization of five-coordinate copper(II) complexes originates from the flexibility of the molecule, in which the interplanar angles of the pyridyl substituents vary within the range 9–42°.

The complexation ability of 2,2′-dipyridylamine is used in several synthetic processes. The addition of hydrocarbons to alkenes in the presence of alkyl mercurials and sodium boranate allows the preparation of ω-phenylalkyl derivatives (Giese & Meister, 1977) and can be expanded to less electrophilic styrenes and allylbenzenes (Grützmacher & Schmuck, 1980). The diphenylboryl complex of 2,2′-dipyridylamine reduces methylviologen and sensitizes the liberation of hydrogen from aqueous alcoholic solutions in the presence of colloidal platinum (Frolov, El'tsov & Ponyaev, 1988).

Boron chelates of 2,2′-dipyridylamine possess antiviral activity, displaying a marked inhibitory effect on both DNA and RNA containing viruses (Lagutkin, Mitin, Zubairov, Dorokhov & Mikhailov, 1982). Highly photoprotective activity and tumour prevention by 2,2′-dipyridylamine is supported by recent studies (Hillebrand, Winslow, Heitmeyer & Bisett, 1990). The tumour-preventive activity of tested iron chelates reaches its maximum with 2,2′-dipyridylamine and supposedly inhibits the iron-catalysed production of oxygen radicals (Hillebrand & Bisett, 1993).

All of the above chemical and biochemical applications of 2,2′-dipyridylamine stimulate a more detailed study of its polymorphs, because these, in general, differ in properties such as melting point, density or solubility. The phenomenon of polymorphism also allows to study structure–property relationships (Bernstein, 1993), because their constant chemical composition reduces the variation of properties exclusively to structural differences. In addition, structural comparison of conformational polymorphs provides insight into the effect of particular intermolecular forces (Bernstein, 1984).

Crystal structures of polymorphic modifications represent distinct local minima on the total energy hypersurface with energy differences ranging usually between 4 and 10 kJ mol^{-1} and, therefore, in the range of activation barriers of rotations about single bonds (Bernstein, 1987; Gavezzotti & Filippini, 1995). Improved insight can be gained by studying phase

transitions and thermodynamic behaviour. Experimental studies on these phenomena are complex and often difficult to reproduce (Dunitz & Bernstein, 1995), but are of general importance. The interest of crystallographers in phase transitions, especially of molecular crystals, therefore, has increased considerably (Dunitz, 1995; Richardson, Yang, Novotny-Bregger & Dunitz, 1990).

2,2′-Dipyridylamine with its two dominant rotational degrees of freedom around the N—C bonds between the amino nitrogen and the pyridyl substituents, and with the two modifications already known, is a prototype molecule to study both structural differences and the crystallization and phase transition behaviour. It has been already noticed in 1923 (Wibaut & Dingemanse, 1923) that 2,2′-dipyridylamine obtained from sodium amide and pyridine melts after recrystallization from aqueous solution at 368 K, which is, thus, ~9° higher than previously reported (Tschitschibabin & Zeide, 1914). This discrepancy, originally explained by impurities, is consistent with the melting points of the two modifications characterized structurally: orthorhombic (Johnson & Jacobson, 1973) and higher melting triclinic (Pyrka & Pinkerton, 1992). At that time, we had already determined the crystal structure of the triclinic modification, and, in addition, investigated different crystallization conditions, and its phase transition by differential thermal analysis and powder diffraction.

In these studies we unexpectedly discovered a third monoclinic modification of 2,2′-dipyridylamine, which transforms only 2° below the melting point of the

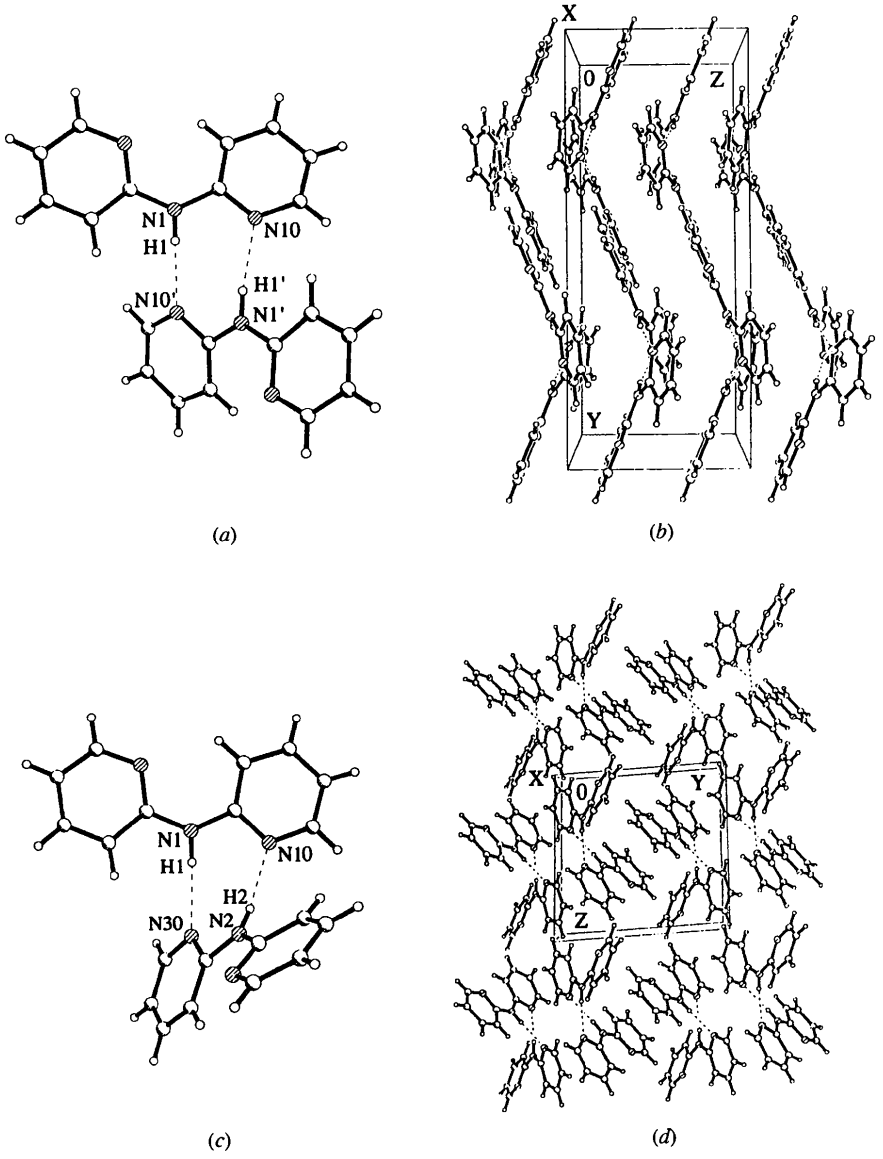

Fig. 1. Orthorhombic 2,2′-dipyridylamine: (*a*) the molecular dimer with twofold crystallographic symmetry and (*b*) view along the *x* direction showing the undulated layers. Triclinic form: (*c*) the stronger twisted hydrogen-bridged dimer and (*d*) the interlocked crystal structure.

triclinic form and, therefore, had not been noticed before. The structure determination of the monoclinic polymorph at 150 K and room temperature, as well as the results of the crystallization and phase transition experiments, are presented here.

1.1. *Orthorhombic and triclinic 2,2′-dipyridylamine*

The low-melting polymorph crystallizes in the orthorhombic space group *Pccn* with eight molecules in the unit cell. Twofold N—H···N-bonded molecular dimers (Fig. 1*a*) are arranged to zigzag-lined layers in the crystallographic *x* direction (Fig. 1*b*). These undulated layers are folded at the hydrogen bonds within the dimers. The central C—N(H)—C units of the hydrogen-bonded dimers are of twofold symmetry and oriented relative to each other with a dihedral angle of 46°. The rotationally unrestricted pyridyl substituents are coplanar to adjacent symmetry equivalents in the *x* direction (Fig. 1*b*).

The crystal structure of the triclinic polymorph comprises two crystallographically independent molecules, which are connected by twofold hydrogen bonding (Fig. 1*c*). In contrast to the orthorhombic form, the hydrogen-bonded molecular dimers, which exhibit a dihedral angle between their C—N(H)—C units of 73°, are oriented almost perpendicular to each other.

The increased indentation of the hydrogen-bonded dimers disturbs the layer arrangement in the orthorhombic polymorph and causes a three-dimensionally interlocked structure (Fig. 1*d*).

2. Experimental

2.1. *Crystallographic studies*

Single crystals of monoclinic 2,2′-dipyridylamine were obtained by transformation of triclinic prisms in acetone solution over 7 d. A colourless prism of dimensions 0.62 × 0.50 × 0.44 mm was mounted on a Siemens P4 diffractometer. Experimental details are summarized in Table 1. Data were corrected for Lorentz and polarization effects. The structure was solved using *SHELXS*86 (Sheldrick, 1985). Refinement on F^2 was accomplished using *SHELXL*93 (Sheldrick, 1993), molecular graphics: *XP* (*SHELXTL/PC*; Sheldrick, 1990).*

All C,N positions were refined with anisotropic displacement parameters. The amino hydrogen was refined with free coordinates and isotropic displacement parameters. All remaining hydrogens were located from difference maps, but positioned with ideal geometry and refined with fixed isotropic displacement parameters using a riding model.

2.2. *Differential thermal analysis (DTA)*

Thermochemical measurements were carried out with a Mettler thermoanalytical TA3000 system with TC10A processor, using aluminum crucibles. The thermocouple element PT100 was calibrated by measuring the melting points of indium (m.p. 429.8 K), lead (m.p. 600.6 K) and zinc (m.p. 692.7 K). The calibration of the heat flux was carried out with a pure indium sample. In all cases the peak maximum temperature is given, because several melting peaks are split.

Optical microscopy was performed with a Kofler heating unit from Wagner & Munz.

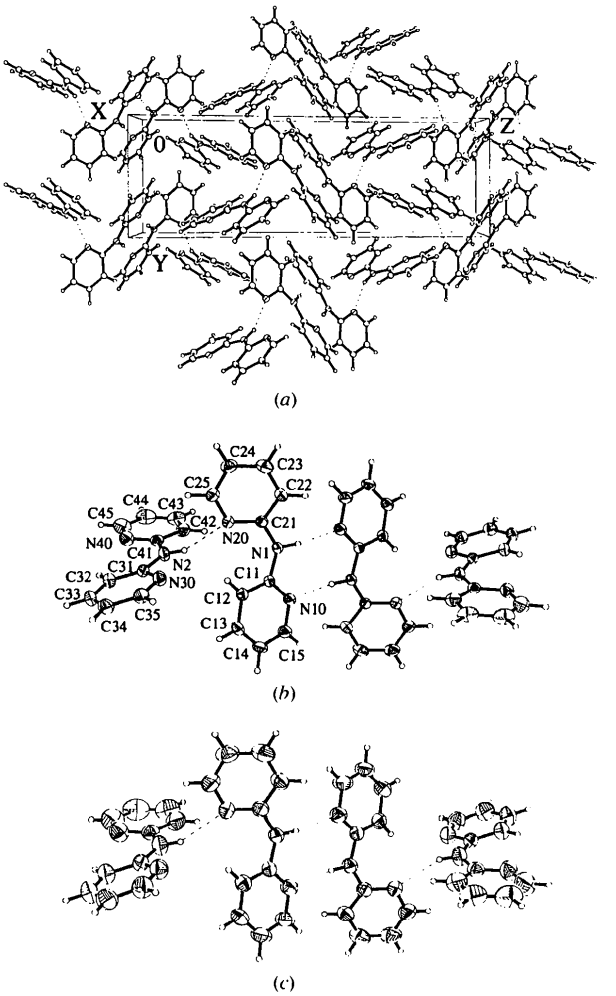

(*a*)

(*b*)

(*c*)

Fig. 2. Crystal structure of monoclinic 2,2′-dipyridylamine: (*a*) interlaced tetrameric hydrogen-bridged units, (*b*) with their displacement ellipsoids at 150 K and (*c*) at room temperature (each at the 50% probability level).

*Lists of structure factors, anisotropic displacement parameters, H-atom coordinates and complete geometry have been deposited with the IUCr (Reference: SE0195). Copies may be obtained through The Managing Editor, International Union of Crystallography, 5 Abbey Square, Chester CH1 2HU, England.

Table 1. *Experimental details*

	150 K	Room temperature
Crystal data		
Chemical formula	$C_{10}H_9N_3$	$C_{10}H_9N_3$
Chemical formula weight	171.20	171.20
Cell setting	Monoclinic	Monoclinic
Space group	$P2_1/c$	$P2_1/c$
a (Å)	8.958 (1)	9.001 (1)
b (Å)	8.161 (1)	8.262 (1)
c (Å)	24.104 (1)	24.234 (1)
β (°)	98.98 (1)	98.88 (1)
V (Å^3)	1740.6 (3)	1780.6 (3)
Z	8	8
D_x (Mg m^{-3})	1.307	1.277
Radiation type	Mo $K\alpha$	Mo $K\alpha$
Wavelength (Å)	0.71073	0.71073
No. of reflections for cell parameters	46	46
θ range (°)	7–20	7–20
μ (mm^{-1})	0.082	0.081
Temperature (K)	150 (2)	293 (2)
Crystal form	Prism	Prism
Crystal size (mm)	0.62 × 0.50 × 0.44	0.62 × 0.50 × 0.44
Crystal colour	Colourless	Colourless
Data collection		
Diffractometer	Siemens P4	Siemens P4
Data collection method	ω scans	ω scans
Absorption correction	None	None
No. of measured reflections	5026	3563
No. of independent reflections	3956	3101
No. of observed reflections	3135	2260
Criterion for observed reflections	$I > 2\sigma(I)$	$I > 2\sigma(I)$
R_{int}	0.0171	0.0202
θ_{max} (°)	27.50	25.00
Range of h, k, l	$-1 \rightarrow h \rightarrow 11$	$0 \rightarrow h \rightarrow 10$
	$0 \rightarrow k \rightarrow 10$	$0 \rightarrow k \rightarrow 9$
	$-31 \rightarrow l \rightarrow 31$	$-28 \rightarrow l \rightarrow 28$
No. of standard reflections	4	4
Frequency of standard reflections	Every 400 reflections	Every 400 reflections
Intensity decay (%)	<1	<1
Refinement		
Refinement on	F^2	F^2
$R[F^2 > 2\sigma(F^2)]$	0.0397	0.0401
$wR(F^2)$	0.1031	0.1058
S	1.022	1.032
No. of reflections used in refinement	3955	3100
No. of parameters used	243	243
H-atom treatment	See text	See text
Weighting scheme	$w = 1/[\sigma^2(F_o^2) + (0.0408P)^2 + 0.4930P]$, where $P = (F_o^2 + 2F_c^2)/3$	$w = 1/[\sigma^2(F_o^2) + (0.0373P)^2 + 0.3432P]$, where $P = (F_o^2 + 2F_c^2)/3$
$(\Delta/\sigma)_{max}$	≤0.001	≤0.001
$\Delta\rho_{max}$ (e Å^{-3})	0.224	0.113
$\Delta\rho_{min}$ (e Å^{-3})	−0.169	−0.132
Extinction method	None	None
Source of atomic scattering factors	*International Tables for Crystallography* (1992, Vol. C, Tables 4.2.6.8 and 6.1.1.4)	*International Tables for Crystallography* (1992, Vol. C, Tables 4.2.6.8 and 6.1.1.4)
Computer programs		
Data collection	*XSCANS*2.10 (Siemens, 1990)	*XSCANS*2.10 (Siemens, 1990)
Cell refinement	*XSCANS*2.10 (Siemens, 1990)	*XSCANS*2.10 (Siemens, 1990)
Data reduction	*XSCANS*2.10 (Siemens, 1990)	*XSCANS*2.10 (Siemens, 1990)
Structure solution	*SHELXS*86 (Sheldrick, 1985)	*SHELXS*86 (Sheldrick, 1985)
Structure refinement	*SHELXL*93 (Sheldrick, 1993)	*SHELXL*93 (Sheldrick, 1993)
Preparation of material for publication	*SHELXL*93–*CIFTAB* (Sheldrick, 1993)	*SHELXL*93–*CIFTAB* (Sheldrick, 1993)

2.3. *Powder diffraction*

The powder diffraction measurements were carried out with a Stoe Stadi P diffractometer with Cu $K\alpha$ radiation ($\lambda = 1.540561$ Å; scan range: $5 \leq 2\theta \leq 40°$; 0.01°).

3. Results and discussion

3.1. *The monoclinic modification of 2,2′-dipyridylamine*

The third and hitherto unknown modification of 2,2′-dipyridylamine crystallizes in the monoclinic space

Table 2. *Fractional atomic coordinates and equivalent isotropic displacement parameters (Å²) for 2,2′-dipyridylamine at 150 K and room temperature*

$U_{eq} = (1/3)\sum_i\sum_j U_{ij}a_i^*a_j^*\mathbf{a}_i.\mathbf{a}_j.$

	x	y	z	U_{eq}
150 K				
N1	−0.34199 (12)	0.45911 (13)	0.45418 (4)	0.0280 (2)
N10	−0.36925 (12)	0.67250 (14)	0.51312 (5)	0.0309 (2)
C11	−0.27970 (13)	0.59981 (15)	0.48066 (5)	0.0241 (2)
C12	−0.13491 (14)	0.6579 (2)	0.47631 (5)	0.0261 (3)
C13	−0.08350 (14)	0.7947 (2)	0.50694 (6)	0.0309 (3)
C14	−0.1737 (2)	0.8707 (2)	0.54097 (6)	0.0358 (3)
C15	−0.3139 (2)	0.8047 (2)	0.54275 (6)	0.0364 (3)
N20	−0.19470 (12)	0.41910 (13)	0.38303 (4)	0.0284 (2)
C21	−0.27633 (13)	0.35433 (15)	0.41936 (5)	0.0244 (2)
C22	−0.30253 (15)	0.1855 (2)	0.42231 (6)	0.0308 (3)
C23	−0.2453 (2)	0.0834 (2)	0.38541 (6)	0.0383 (3)
C24	−0.1610 (2)	0.1492 (2)	0.34729 (6)	0.0403 (3)
C25	−0.1377 (2)	0.3160 (2)	0.34838 (6)	0.0349 (3)
N2	−0.08120 (12)	0.71748 (14)	0.32975 (5)	0.0300 (2)
N30	0.13786 (13)	0.68009 (14)	0.38962 (4)	0.0312 (2)
C31	0.07076 (14)	0.75635 (15)	0.34300 (5)	0.0255 (3)
C32	0.14798 (15)	0.8666 (2)	0.31321 (6)	0.0321 (3)
C33	0.2995 (2)	0.8941 (2)	0.33246 (6)	0.0372 (3)
C34	0.3704 (2)	0.8138 (2)	0.37979 (6)	0.0375 (3)
C35	0.2849 (2)	0.7094 (2)	0.40659 (6)	0.0355 (3)
N40	−0.14212 (14)	0.8312 (2)	0.23975 (5)	0.0376 (3)
C41	−0.18691 (14)	0.7570 (2)	0.28350 (5)	0.0279 (3)
C42	−0.3385 (2)	0.7170 (2)	0.28532 (6)	0.0379 (3)
C43	−0.4452 (2)	0.7591 (2)	0.24071 (7)	0.0492 (4)
C44	−0.4010 (2)	0.8392 (2)	0.19520 (7)	0.0522 (4)
C45	−0.2504 (2)	0.8702 (2)	0.19647 (7)	0.0489 (4)
Room temperature				
N1	−0.3412 (2)	0.4603 (2)	0.45443 (6)	0.0499 (4)
N10	−0.3689 (2)	0.6715 (2)	0.51243 (6)	0.0552 (4)
C11	−0.2798 (2)	0.5998 (2)	0.48041 (6)	0.0425 (4)
C12	−0.1368 (2)	0.6570 (2)	0.47612 (6)	0.0466 (4)
C13	−0.0864 (2)	0.7918 (2)	0.50598 (7)	0.0571 (5)
C14	−0.1758 (2)	0.8671 (2)	0.53939 (8)	0.0660 (5)
C15	−0.3135 (2)	0.8024 (2)	0.54128 (8)	0.0676 (6)
N20	−0.1969 (2)	0.4211 (2)	0.38320 (5)	0.0504 (4)
C21	−0.2771 (2)	0.3570 (2)	0.41938 (6)	0.0434 (4)
C22	−0.3029 (2)	0.1915 (2)	0.42217 (8)	0.0550 (4)
C23	−0.2469 (2)	0.0914 (2)	0.38546 (9)	0.0695 (5)
C24	−0.1640 (2)	0.1564 (3)	0.34774 (9)	0.0727 (6)
C25	−0.1409 (2)	0.3190 (3)	0.34881 (8)	0.0643 (5)
N2	−0.0813 (2)	0.7203 (2)	0.32969 (6)	0.0551 (4)
N30	0.1364 (2)	0.6823 (2)	0.38881 (6)	0.0567 (4)
C31	0.0701 (2)	0.7587 (2)	0.34280 (6)	0.0456 (4)
C32	0.1468 (2)	0.8673 (2)	0.31396 (7)	0.0579 (5)
C33	0.2963 (2)	0.8936 (3)	0.33299 (9)	0.0692 (6)
C34	0.3666 (2)	0.8141 (3)	0.37943 (9)	0.0684 (5)
C35	0.2824 (2)	0.7112 (3)	0.40551 (8)	0.0650 (5)
N40	−0.1419 (2)	0.8348 (2)	0.24093 (6)	0.0679 (4)
C41	−0.1864 (2)	0.7598 (2)	0.28378 (7)	0.0496 (4)
C42	−0.3357 (2)	0.7185 (3)	0.28524 (8)	0.0664 (5)
C43	−0.4412 (2)	0.7593 (3)	0.24115 (11)	0.0850 (7)
C44	−0.3980 (3)	0.8397 (3)	0.19678 (11)	0.0919 (7)
C45	−0.2490 (3)	0.8728 (3)	0.19822 (9)	0.0887 (7)

group $P2_1/c$ with eight molecules in the unit cell (Fig. 2, Tables 1 and 2). In contrast to both forms already reported (Johnson & Jacobson, 1973; Pyrka & Pinkerton, 1992) its crystal structure is characterized by hydrogen-bonded tetramers (Fig. 2*b*). The central motif of the known orthorhombic and triclinic twofold hydrogen-bonded dimers is located around a centre of inversion. The second, in both other cases uncoordinated, pyridyl nitrogen accepts an additional single N—H···N hydrogen bond, from another crystallographically independent molecule. Neither pyridyl nitrogens of this additional dipyridylamine are involved in any hydrogen bonds. Consequently, there is one N—H···N hydrogen bond per molecule, analogous to the other two modifications.

The view in the *x* direction (Fig. 2*a*) shows the interlocked arrangement of the tetrameric aggregates. The planes of the central C—N(H)—C units of the hydrogen-bonded dimers with a centre of inversion between them are not twisted relative to each other. The 2-aminopyridyl fragments connected by a pair of hydrogen bonds are not coplanar, but shifted by 0.51 Å perpendicular to each other. The refined H-atom position H1 is located 0.20 Å above the central C—N—C plane and oriented into the direction of the hydrogen-bond-accepting pyridyl nitrogen N10′. The pyridyl substituent is largely located within this plane, deviating by a dihedral angle of 3°. On the contrary, the second pyridyl ring is rotated 38° out of this plane. The N—H···N hydrogen bonds from both the additional dipyridylamines expand the central dimer motif to a tetrameric one. Their idealized molecular planes are oriented with angles of 80° close to perpendicular with respect to the central dimer (Fig. 2*c*). This arrangement allows for the necessary spatial proximity to accommodate a hydrogen bond between them. In addition, a layer formation is prevented by this orientation and, therefore, an interlaced crystal structure results.

The N—H···N hydrogen bonds exhibit almost identical N···N distances of 3.00 and 3.02 Å. The N1—H1···N10′ bond of the cooperatively connected central unit (Fig. 3*a*) is almost linear with the NHN angle 172°. In contrast, the N2—H2···N20 single bond (Fig. 3*b*) exhibits an angle of only 157°. Packing effects presumably enforce the orientation of the outer molecule and, thereby, of its hydrogen bond.

The amino N1 atom with a 359° sum of angles deviates slightly from planarity due to the alignment of H1, whereas the bonds around N2 are strictly planar. The outer dipyridylamine exhibits an interplanar angle between its pyridyl rings of 14° and, therefore, is considerably less distorted than the central one twisted by 38°. The hydrogen-bond-free pyridyl substituents of the outer molecule are rotated in opposite directions by 7 and 8° out of the C—N—C plane in between them (Fig. 3*d*).

The central C11—N1—C21 and C31—N2—C41 angles of both independent 2,2′-dipyridylamines are widened to 128 and 131°, presumably due to intramolecular C—H···N interactions between the pyridyl substituents, which should be stronger in the more planar molecule. Both independent molecules exhibit reduced (H)N—C—N angles to the *trans*-situated pyridyl nitrogen (Table 3). The published speculation (Johnson & Jacobson, 1973) that this effect could be a consequence of the hydrogen bonding between the

Table 3. *Bond lengths (Å) and angles (°) for monoclinic 2,2'-dipyridylamine at 150 K [in square brackets at room temperature]*

N1—C11	1.388 (2)	[1.387 (2)]	N2—C41	1.384 (2)	[1.384 (2)]
N1—C21	1.391 (2)	[1.390 (2)]	N2—C31	1.386 (2)	[1.388 (2)]
N10—C11	1.343 (2)	[1.337 (2)]	N30—C35	1.338 (2)	[1.336 (2)]
N10—C15	1.345 (2)	[1.342 (2)]	N30—C31	1.342 (2)	[1.339 (2)]
C11—C12	1.400 (2)	[1.390 (2)]	C31—C32	1.399 (2)	[1.385 (2)]
C12—C13	1.378 (2)	[1.367 (2)]	C32—C33	1.382 (2)	[1.371 (3)]
C13—C14	1.384 (2)	[1.375 (2)]	C33—C34	1.381 (2)	[1.371 (3)]
C14—C15	1.374 (2)	[1.357 (3)]	C34—C35	1.373 (2)	[1.358 (3)]
N20—C21	1.335 (2)	[1.329 (2)]	N40—C41	1.331 (2)	[1.323 (2)]
N20—C25	1.341 (2)	[1.338 (2)]	N40—C45	1.347 (2)	[1.338 (3)]
C21—C22	1.401 (2)	[1.391 (2)]	C41—C42	1.404 (2)	[1.392 (2)]
C22—C23	1.375 (2)	[1.367 (2)]	C42—C43	1.366 (2)	[1.358 (3)]
C23—C24	1.385 (2)	[1.375 (3)]	C43—C44	1.387 (3)	[1.370 (3)]
C24—C25	1.377 (2)	[1.359 (3)]	C44—C45	1.368 (2)	[1.364 (3)]
N1—H1	0.92 (2)	[0.90 (2)]	N20—H2	2.18 (2)	[2.27 (2)]
N2—H2	0.87 (2)	[0.84 (2)]	N1—N10^{i}	3.017 (1)	[3.048 (2)]
N10^{i}—H1	2.10 (2)	[2.15 (2)]	N2—N20	3.003 (2)	[3.048 (2)]
C11—N1—C21	127.5 (1)	[127.9 (1)]	C41—N2—C31	131.0 (1)	[131.0 (2)]
C11—N10—C15	117.4 (1)	[116.9 (1)]	C35—N30—C31	117.7 (1)	[117.3 (2)]
N10—C11—N1	113.6 (1)	[113.5 (1)]	N30—C31—N2	112.5 (1)	[112.2 (1)]
N10—C11—C12	122.6 (1)	[122.5 (2)]	N30—C31—C32	122.4 (1)	[122.2 (2)]
N1—C11—C12	123.8 (1)	[123.9 (1)]	N2—C31—C32	125.1 (1)	[125.5 (2)]
C13—C12—C11	118.1 (1)	[118.3 (2)]	C33—C32—C31	118.1 (1)	[118.2 (2)]
C12—C13—C14	120.2 (1)	[120.2 (2)]	C34—C33—C32	120.1 (1)	[120.3 (2)]
C15—C14—C13	117.7 (1)	[117.5 (2)]	C35—C34—C33	117.7 (1)	[117.5 (2)]
N10—C15—C14	124.1 (1)	[124.6 (2)]	N30—C35—C34	124.2 (1)	[124.4 (2)]
C21—N20—C25	117.5 (1)	[117.1 (2)]	C41—N40—C45	116.8 (1)	[116.6 (2)]
N20—C21—N1	118.6 (1)	[118.5 (2)]	N40—C41—N2	119.4 (1)	[119.3 (2)]
N20—C21—C22	122.4 (1)	[122.4 (2)]	N40—C41—C42	122.9 (1)	[123.0 (2)]
N1—C21—C22	118.9 (1)	[119.1 (2)]	N2—C41—C42	117.7 (1)	[117.7 (2)]
C23—C22—C21	118.7 (1)	[118.8 (2)]	C43—C42—C41	118.5 (2)	[118.7 (2)]
C22—C23—C24	119.4 (1)	[119.3 (2)]	C42—C43—C44	119.4 (2)	[119.3 (2)]
C25—C24—C23	117.9 (1)	[118.1 (2)]	C45—C44—C43	118.1 (2)	[118.3 (2)]
N20—C25—C24	124.1 (1)	[124.3 (2)]	N40—C45—C44	124.2 (2)	[124.1 (2)]
N1—H1—N10^{i}	172 (1)	[172 (2)]	N2—H2—N20	157 (2)	[156 (2)]

Symmetry code: (i) $-x-1, 1-y, 1-z$.

central moieties, therefore, cannot be supported, because the outer molecule, which does not participate in twofold hydrogen bonding, exhibits the same distortion caused by the intramolecular C—H···N interaction. All structural parameters are listed in Table 3.

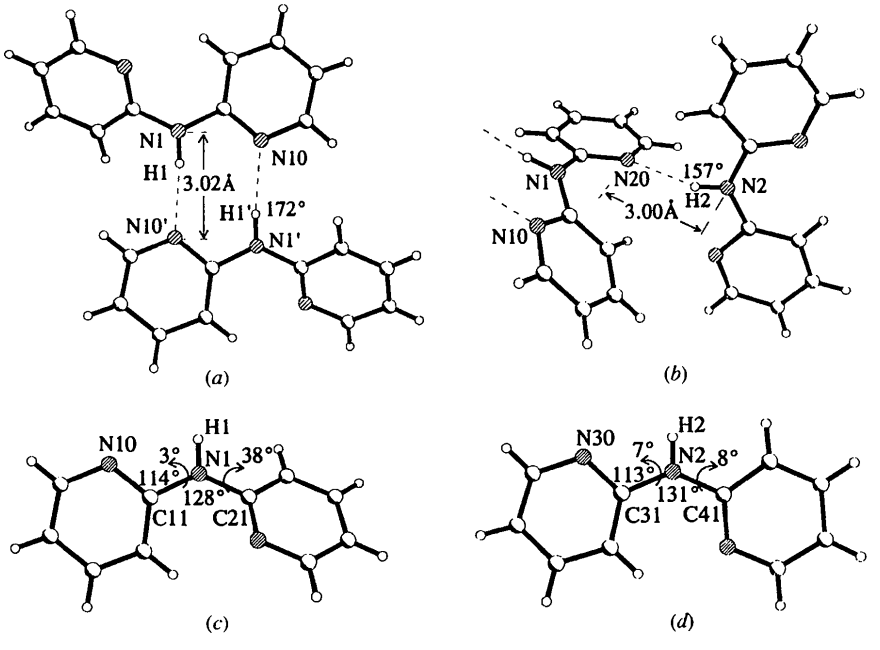

Fig. 3. Hydrogen bonds in monoclinic 2,2'-dipyridylamine and selected structural parameters: (*a*) central hydrogen-bridged dimer, (*b*) additionally connected dipyridylamine with hydrogen bridge N2—H2···N20, considerably deviating from linearity, and (*c*) and (*d*) two independent molecules with different torsional angles, but almost identical distances.

3.2. *Comparison of the polymorphic crystal structures*

The essential structural motif of the twofold hydrogen-bonded dimer in all three modifications of 2,2′-dipyridylamine is characterized by its extraordinary flexibility. The relative orientations of the central C—N(H)—C planes vary over the range 70°. The parallel planes observed in the monoclinic structure, therefore, can be distorted up to 73° without damage to the cooperative hydrogen bonding, as demonstrated by the triclinic dimer (Fig. 4*a*). The orthorhombic modification with its interplanar angle of 46° is intermediate between these extremes (Fig. 4*b*). The marked flexibility of the twofold hydrogen-bonded moiety (Fig. 4*d*) is further supported by the observation that the accepting pyridyl ring rotates around the N—C bond between the amino nitrogen and pyridyl substituent to keep the maximum hydrogen-bond alignment: For instance, the pyridyl ring rotation by a negligible angle of 3° in the monoclinic dimer is enlarged to 16° in the orthorhombic form. In the triclinic modification, with its strong distortion, the relatively small rotations of the hydrogen-bonded pyridyl substituents cause considerable deviations of the N—H vector out of the nitrogen lone-pair axis of the other hydrogen-bonded nitrogen by 43 and 26°. In contrast, the N—H vector deviates from the lone-pair axis by only 17° in the monoclinic and 10° in the orthorhombic modification.

Distances and angles of the hydrogen bonds in all dimeric units are largely comparable in the three modifications. The N···N distances range from 3.00 to 3.06 Å and the NHN angles from 170 to 176°. The molecular structures of 2,2′-dipyridylamine differ primarily in the torsion angles of their pyridyl substituents, which vary between 3 and 38°. These extreme values are both observed in the central molecule of the novel tetramer in the monoclinic polymorph. The interplanar angle of the pyridyl substituents within one dipyridylamine ranges between 8 and 39°. The central C—N—C angles, widened in all polymorphs, are determined within 128–131°. The N(H)—C—N angle involving the *trans*-configurated pyridyl nitrogen is reduced to 113 ± 1° in all cases. All other structural data vary only little.

3.3. *Thermal investigations*

On heating an orthorhombic single crystal to ~323 K, initial changes in the phenotype of the crystal are observed. Starting at crystal defects, several waves move through the crystal, accompanied by a loss of transparency and the formation of cracks. The wave-like distortion progresses preferentially in the direction of the needle axis [001]. X-ray measurement proves that a polycrystalline material results. Further heating establishes a melting point of ~369 K.

Supporting these optical observations, differential thermal analysis measurements (DTA) show an endothermic peak between 323 and 360 K and a second endothermic peak at 369 K, which corresponds to the melting point of the transformation product (Fig. 5:

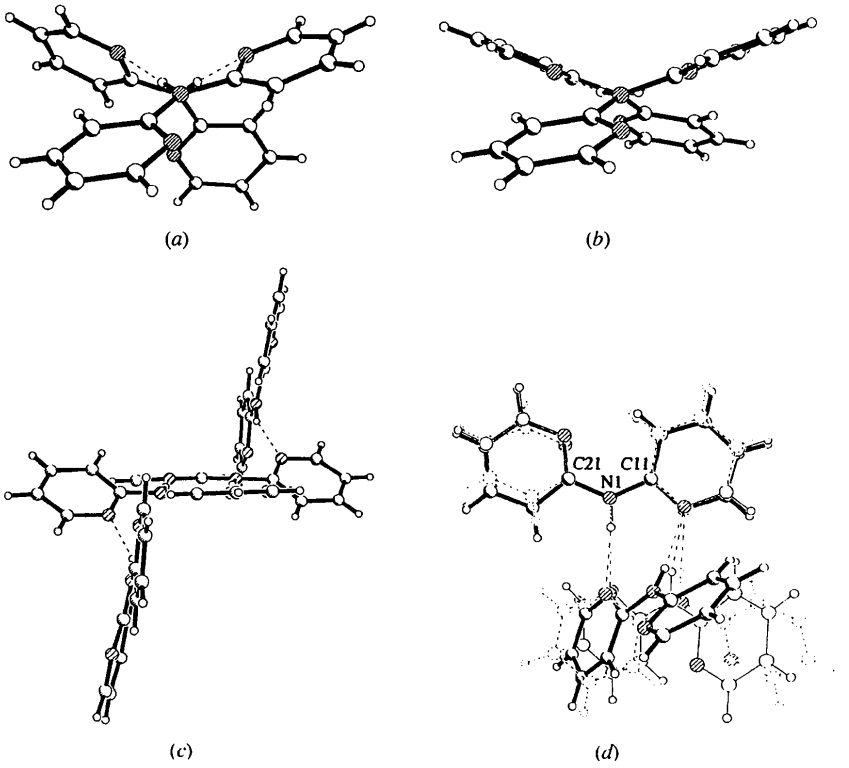

Fig. 4. Different orientations of hydrogen-bridge-connected 2,2′-dipyridylamine subunits in the individual modifications: (*a*) triclinic form with a maximum twisting of 73°, (*b*) orthorhombic dimer with its 46° distortion, (*c*) central unit of the monoclinic tetramer without any torsion and (*d*) projection of the three different orientations after fitting the positions N1, C11 and C21 of the triclinic (—), orthorhombic (—) and monoclinic (---) modifications.

curves 1, 3 and 6). The shape and width of the transformation peak, as well as the transition temperature, depends on the heating rate and crystal quality. Low heating rates result in well shaped peaks, whereas faster rates generate broad and flat peaks, which are hardly detectable. If the heating is interrupted at 353 K and heating repeated after cooling down to 283 K, no transformation peak will be detected (Fig. 5: curve 6).

By lowering the temperature, the melt shows a supercooling effect down to 318 K (Fig. 5: curve 2). On repeated heating of the solidified melt, the sample transforms again, as indicated by a broad and flat peak (Fig. 5: curve 3); in some cases an additional sharp peak at 360 K is observed. This experiment can be repeated infinitely using the same sample with and without the occurrence of the additional peak. Its temperature corresponds to the melting point of the orthorhombic form reported in the literature (Johnson & Jacobsen, 1973) and, thus, should be due to some unchanged orthorhombic material. Consequently, the observed irreversible destruction of the single crystal during the transformation should be reconstructive and, therefore, of first order. According to the literature (Mnyukh, 1979), such a transformation usually exhibits hysteresis behaviour and, thereafter, a melting process without any transformation should be possible. This phenomenon is in accord with the additional peak sometimes observed in the DTA experiments.

The transformation product is characterized by powder diffraction methods (Fig. 6). The resulting diagram proves to be a superposition of the calculated patterns of all three modifications. In addition, powder diffraction patterns of melted samples have been registered, which were either cooled down slowly or

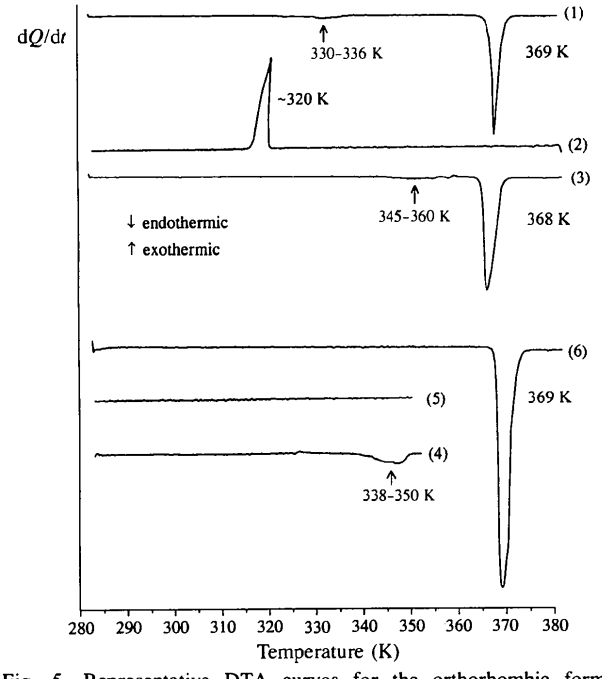

Fig. 5. Representative DTA curves for the orthorhombic form measured between 283 and 383 K (heating rate 2 K min^{-1}), 11.1 mg single crystal: (1) heating curve, (2) cooling curve and (3) repeated heating curve; and with 15.4 mg single crystal: (4) heating curve from 283 to 353 K, (5) cooling to 283 K and (6) repeated heating curve from 283 to 383 K.

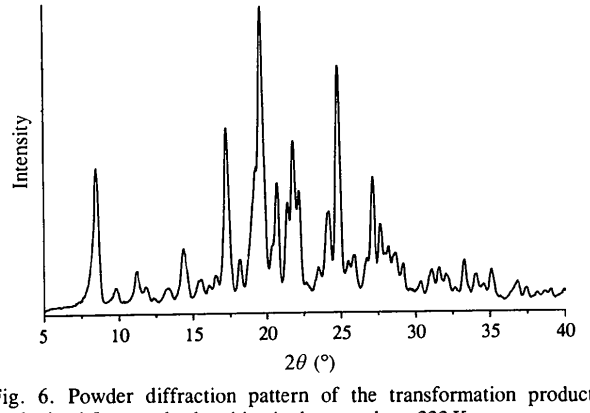

Fig. 6. Powder diffraction pattern of the transformation product obtained from orthorhombic single crystals at 333 K.

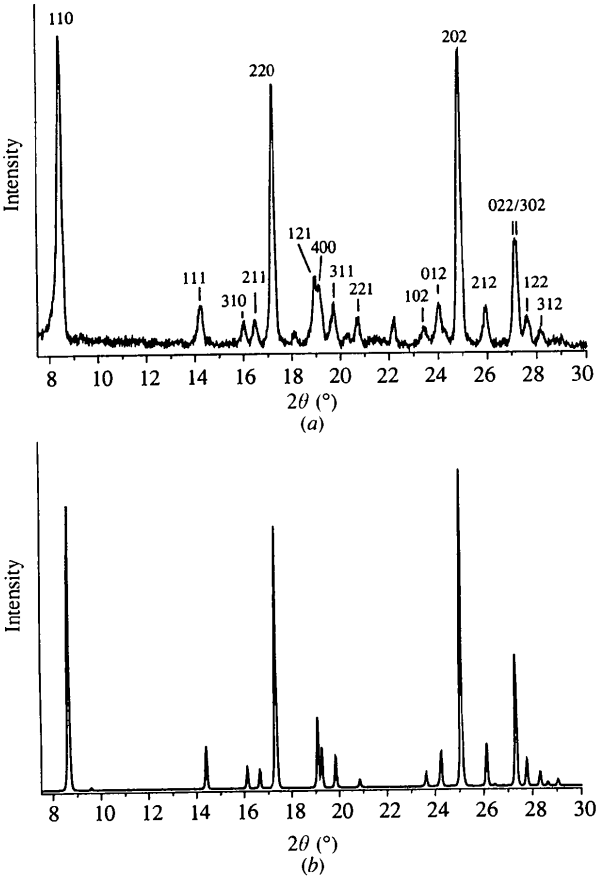

Fig. 7. Powder diffraction pattern (*a*) determined experimentally for the solidified melt and (*b*) the identical calculated pattern for the orthorhombic modification.

frozen rapidly by liquid nitrogen (Fig. 7*a*). All prove to be identical to the pattern calculated for the orthorhombic form (Fig. 7*b*).

The DTA diagram for the monoclinic modification exhibits a broad peak with a minimum at 370 K and, depending on the heating rate, sometimes an additional small separated peak at ~368 K (Fig. 8*a*: ⇓). For further information concerning this unexpected observation, the respective monoclinic single crystals were heated to 368 K under optical control by a Kofler microscope and kept at this temperature just below the melting point. After a period of ~10 min the slow movement of one distinct transformation wave through the whole crystal was observed. The crystal cracked at several spots and lost its transparency. The analysis of the residual material by powder diffraction yielded a pattern (Fig. 9*a*), which completely resembled the calculated pattern for the triclinic modification (Fig. 9*b*).

In addition, a monoclinic single crystal has been tempered at 368 K until the wave-like change is observed and tested by X-ray diffraction, which proved the loss of its single crystallinity and its change to polycrystalline material. In contrast, analogous DTA experiments with triclinic crystals (Fig. 8*b*) do not provide any evidence of phase transformation, but result in a sharp melting peak close to 370 K (Fig. 8*b*: curve 3).

3.4. *Crystal growth and morphology*

Single crystals of 2,2′-dipyridylamine were grown in different solvents and also by sublimation, which yields the triclinic modification exclusively. All three modifications can be obtained by crystallization from acetone solution. On slow solvent evaporation at room temperature, first colourless needles of the orthorhombic form grow. The rectangular needles with the needle axis along [001] possess either squaric faces (001) or a plate-like habit achieved by an elongation of the [1$\bar{1}$0] crystal axis (Fig. 10*b*). Simultaneously, or up to 1 h later, nuclei of triclinic crystals form and start growing at the cost of the orthorhombic needles, which finally disappear completely. The triclinic crystals are polyhedral (Fig. 10*c*) and on further standing of the acetone solution, rhombohedrally shaped crystals start to grow.

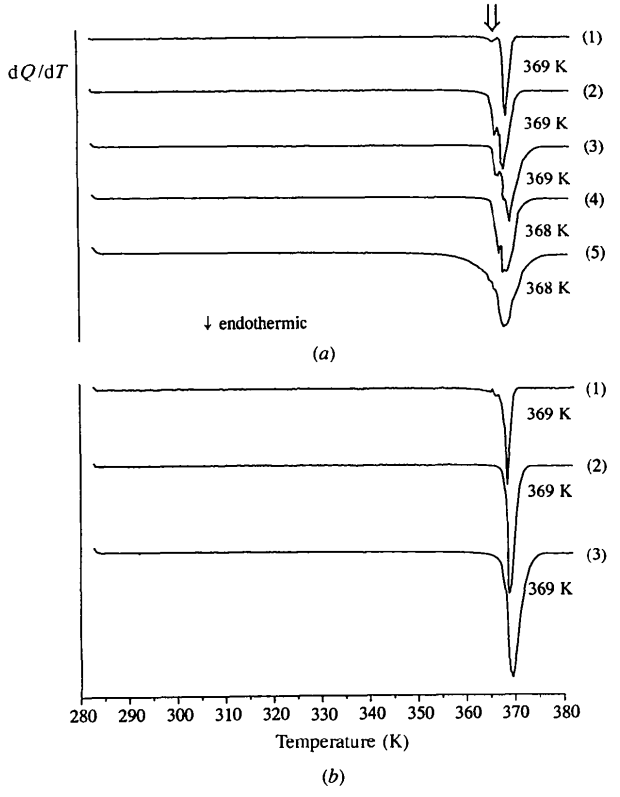

Fig. 8. DTA heating curves at different heating rates between 283 and 383 K. (*a*) Monoclinic 2,2′-dipyridylamine (fragments of the same single crystal): (1) m.p. 369 K (1 K min^{-1}; 11.6 mg), (2) m.p. 369 K (2 K min^{-1}; 15.3 mg), (3) m.p. 369 K (3 K min^{-1}; 20.3 mg), (4) m.p. 368 K (4 K min^{-1}; 13.8 mg) and (5) m.p. 368 K (5 K min^{-1}; 20.5 mg). (*b*) Triclinic 2,2′-dipyridylamine (single crystals): (1) m.p. 369 K (1 K min^{-1}; 9.8 mg), (2) m.p. 369 K (2 K min^{-1}; 13.1 mg) and (3) m.p. 369 K (3 K min^{-1}; 19.1 mg).

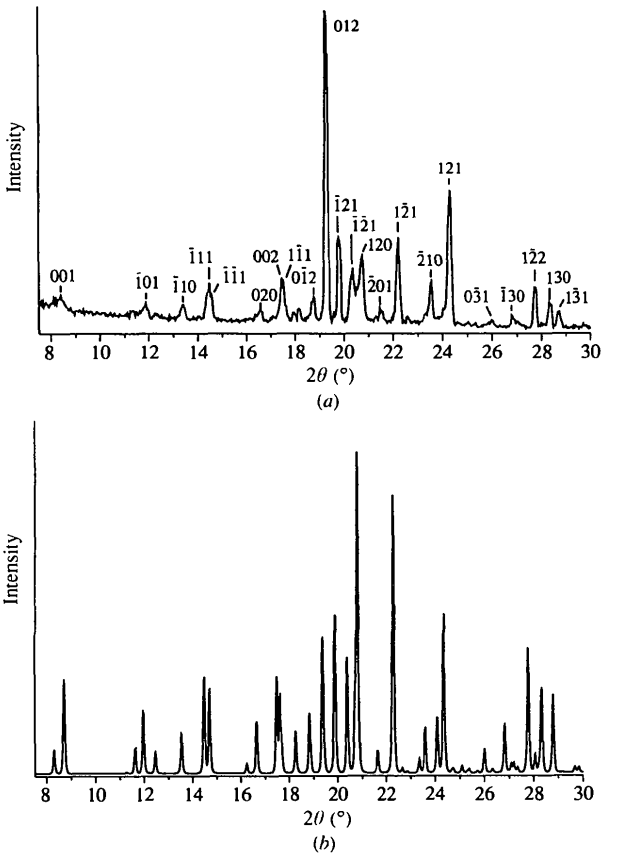

Fig. 9. Powder diffraction pattern (*a*) of the transformation product of a monoclinic single crystal at 368 K and (*b*) the identical calculated pattern for triclinic 2,2′-dipyridylamine.

At least 5 h after the appearance of the first crystals, all the triclinic crystals are replaced by those of the monoclinic modification. The appearance of monoclinic prisms (Fig. 10*a*) often requires several days.

3.5. *Thermodynamic aspects*

The stability sequence of the three modifications has been investigated by competing crystallization of two of each single crystal of different forms in saturated acetone solution. The relative stabilities determined coincide with the order of crystallization on slow solvent evaporation at room temperature described above. Monoclinic single crystals grow at the cost of the triclinic as well as the orthorhombic form and, therefore, should represent the most stable modification at this temperature. An orthorhombic single crystal dissolves in favour of the triclinic crystal, indicating less thermodynamic stability. These experiments have been carried out in several solvents, such as toluene, ethanol and diethyl ether, and always result in the same stability order. The crystals obtained are each easily identified by their characteristic crystal habits (Fig. 10) and the results confirmed by determination of the cell or by a comparison of the powder diffraction patterns.

The investigation behaviour and the resulting stability order observed by the DTA investigation seem to contradict the results obtained from the crystallization experiments: According to the endothermic transformation peak in the range 330–336 K (Fig. 5: 1), the orthorhombic modification should be the most stable at room temperature. This assumption is further supported by its highest density and lowest melting point. With regard to the known phenomenon of hysteresis (Mnyukh, 1979), the real transition point is very often at signficantly lower temperature and, therefore, additional stability experiments in solution have been performed at several temperatures below 293 K. Both at 283 and 273 K, the stability order does not change. However, by storing the three crystal forms of 2,2′-dipyridylamine in acetone solution at 263 and 248 K for several days, the orthorhombic single crystals grow at the cost of all others and, therefore, appear to be the most stable modification at lower temperatures. The resulting low-temperature stability sequence is in accordance with the order of crystal densities. The thermodynamic transition point should be located in between 263 and 273 K.

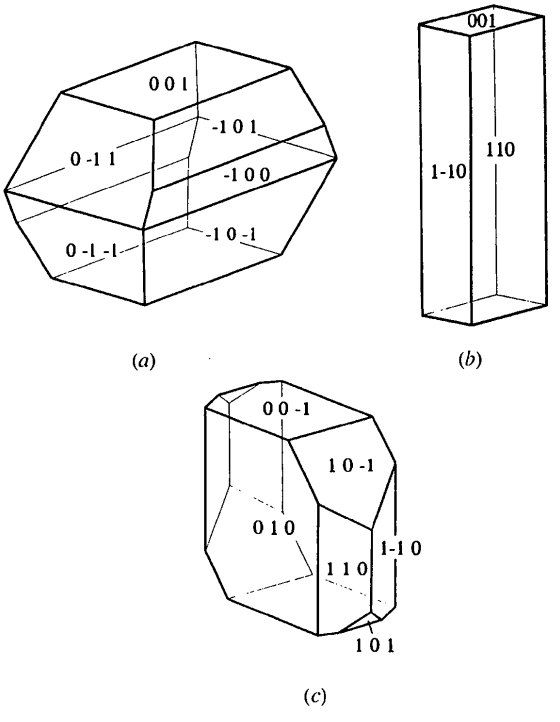

Fig. 10. Crystal shapes with indexed faces: (*a*) monoclinic prism, (*b*) orthorhombic needle and (*c*) polyhedral triclinic rhombus.

Analogous investigations on the second-phase transition from the monoclinic to the triclinic modification, observed optically and by DTA measurements just below the melting point, were carried out at several temperatures between room temperature and the melting point: The saturated solution of 2,2′-dipyridylamine in ethanol containing a crystalline sediment was stirred for ~20 h at a specific temperature. From the initially microcrystalline material a number of crystals grew within hours and then remained unchanged. Monoclinic single crystals were obtained at 293 and 303 K, whereas triclinic ones were isolated at temperatures of 313 K and above. Therefore, the respective thermodynamic transition point is expected between 303 and 313 K.

A comparison of the temperature dependence of the cell volumes (Table 4, normalized to eight formula units) provides interesting information (Fig. 11): The orthorhombic modification exhibits by far the lowest volume and the highest density over the whole temperature range tested. According to an empirical rule, the internal energy of a polymorph decreases with increasing density and only a few exceptions are known, especially for hydrogen-bonded networks (Dunitz, 1995). The volumes of the triclinic and monoclinic modifications are almost conformable. Between 270 and 290 K, the triclinic form becomes that with the highest volume at higher temperatures (Fig. 11). The slight deviation below the crossing point between the monoclinic and triclinic forms could originate from their different hydrogen-bond motifs or from differences in their molecular free energies.

The experimental results allow an estimation of the temperature dependence of the relative free energies for all three modifications of 2,2′-dipyridylamine (Fig. 12).

Table 4. *Temperature-dependent cell constants for the three modifications of 2,2′-dipyridylamine*

	130 K	180 K	230 K	280 K	300 K	320 K
(*a*) Orthorhombic						
a (Å)	18.431 (2)	18.432 (1)	18.429 (1)	18.423 (1)	18.419 (1)	
b (Å)	12.202 (1)	12.219 (1)	12.250 (1)	12.278 (1)	12.289 (1)	
c (Å)	7.533 (1)	7.562 (1)	7.634 (1)	7.704 (1)	7.735 (1)	
V (Å^3)	1694.0 (6)	1703.2 (2)	1723.3 (3)	1742.6 (3)	1750.8 (3)	
(*b*) Monoclinic						
a (Å)	8.956 (1)	8.968 (1)	8.983 (1)	9.001 (1)	9.007 (1)	9.019 (1)
b (Å)	8.152 (1)	8.180 (1)	8.214 (1)	8.256 (1)	8.271 (1)	8.292 (1)
c (Å)	24.108 (3)	24.158 (3)	24.202 (3)	24.252 (3)	24.266 (3)	24.291 (3)
β (°)	99.01 (1)	98.97 (1)	98.92 (1)	98.88 (1)	98.87 (1)	98.85 (1)
V (Å^3)	1738.4 (7)	1750.7 (6)	1764.3 (6)	1780.7 (5)	1786.2 (6)	1795.1 (7)
(*c*) Triclinic						
a (Å)	8.176 (3)	8.195 (3)	8.216 (3)	8.231 (3)	8.244 (4)	8.275 (3)
b (Å)	10.520 (2)	10.561 (2)	10.610 (2)	10.659 (2)	10.699 (4)	10.727 (2)
c (Å)	10.578 (3)	10.603 (3)	10.631 (3)	10.655 (2)	10.682 (4)	10.691 (3)
α (°)	92.83 (1)	92.83 (2)	92.86 (1)	92.89 (1)	92.84 (2)	92.93 (1)
β (°)	107.06 (1)	107.15 (1)	107.26 (1)	107.37 (1)	107.49 (2)	107.59 (1)
γ (°)	93.32 (1)	93.24 (1)	93.18 (1)	93.09 (1)	93.08 (2)	92.99 (1)
V (Å^3)	866.2 (8)	873.4 (8)	881.5 (8)	888.7 (7)	895.2 (9)	901.2 (8)

Obviously, the triclinic form is thermodynamically most stable above ~310 K. Between 270 and 310 K the monoclinic modification should exhibit the highest stability and below 270 K the orthorhombic form is supposedly the most stable. According to these results, the possibility of an additional modification at lower temperature cannot be excluded.

4. Conclusions

Macroscopically the three modifications of 2,2′-dipyridylamine, including the novel monoclinic one (Fig. 2), differ significantly in both their densities ρ and their melting points m.p. (Table 5), which can be qualitatively correlated with the crystal structures. The orthorhombic form (Fig. 1*b*), due to its undulated layers, possesses a distinctly higher density than the other modifications. The triclinic modification, lacking any layer-like substructure, is less efficiently packed (Fig 1*d*) and the almost perpendicular arrangement of molecules in tetrameric units (Fig. 4*c*) in the monoclinic crystal structure (Fig. 2*a*) causes the lowest density of all. On the other hand, the interlocked arrangements in both the triclinic and monoclinic crystal forms give rise to significantly higher melting points compared with the more flexible layers of the orthorhombic form.

On comparison of the three crystal structures, it becomes obvious that the structural changes during the transformations have to be accompanied by extreme rotational and translational movements and, therefore, tend to destroy the single crystal. The optical observations suggest a mechanism, which originates at crystal defects and is controlled by nucleation and growth of the new phase. This mechanism is supported by the hysteresis detected in the DTA experiments and places the transformation temperature within the range where the free energy curves of the triclinic and monoclinic modifications cross each other. Therefore, it can be rationalized that the transformation of orthorhombic crystals results in a mixture of all three modifications. The persistance of unchanged orthorhombic crystals can be explained by the assumption that each defect, suitable of nucleation of a new phase, should have its

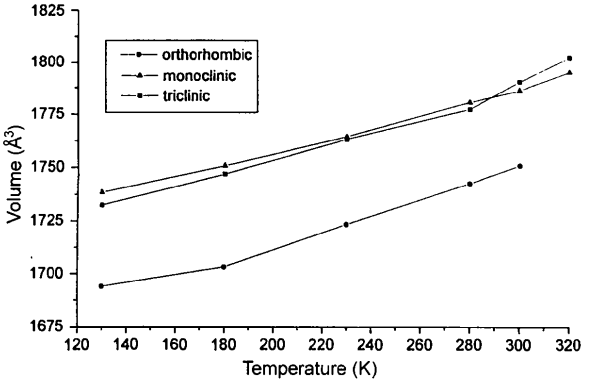

Fig. 11. Temperature dependence of the cell volume, normalized to $Z = 8$, for the three modifications of 2,2′-dipyridylamine (at 320 K the cell volume of the orthorhombic crystal cannot be determined due to its destructive transformation).

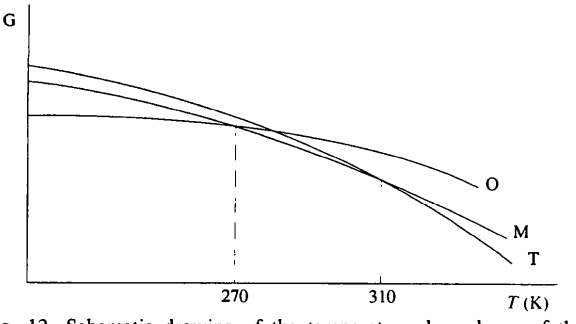

Fig. 12. Schematic drawing of the temperature dependence of the three energies for the three modifications of 2,2′-dipyridylamine.

Table 5. *Crystal and physical data for the three polymorphs of 2,2′-dipyridylamine at room temperature*

	Orthorhombic	Monoclinic	Triclinic
Space group	*Pccn*	$P2_1/c$	$P\bar{1}$
Z	8	8	4
M.p. (K)	360	~369	369
ρ (g cm^{-3})	1.343	1.307	1.318

own characteristic 'pre-coded' transition temperature, which is variable and finally can suppress the transformation (Mnyukh, 1979).

Summarizing, this contribution to the remarkable phenomenon of polymorphism further substantiates the importance of knowledge on the existence and thermodynamic stability of all polymorphic modifications. Relationships between crystal structures on one hand and the interconversions of polymorphic modifications on the other are of principal importance and, therefore, additional investigations to improve their understanding are indispensable. To continue a systematic approach, it should be advantageous to study slightly modified systems. Therefore, and stimulated by the results for 2,2′-dipyridylamine, we have started to investigate with 2-pyridyl(2′-pyrimidyl)amine.

The project is supported by the Deutsche Forschungsgemeinschaft, the State of Hesse, the Fonds der Chemischen Industrie, the Hoechst Corporation and the A. Messer Foundation. We gratefully thank Professor K. Hensen from the Institute of Physical Chemistry of Frankfurt/Main for providing us with his DTA device.

References

Bernstein, J. (1984). *X-ray Crystallography and Drug Action* edited by A. S. Horn & C. J. De Ranter, pp. 23–44. Oxford: Clarendon Press.

Bernstein, J. (1987). *Organic Solid State Chemistry*, edited by G. R. Desiraju, pp. 471–518. Amsterdam: Elsevier.

Bernstein, J. (1993). *J. Phys. D*, **26**, B66–B76.

Dunitz, J. D. (1995). *Acta Cryst.* B**51**, 619–631.

Dunitz, J. D. & Bernstein, J. (1995). *Acc. Chem. Res.* **28**, 193–200.

Frolov, A. N., El'tsov, A. V. & Ponyaev, A. I. (1988). *Zh. Obshch. Khim.* **58**, 1685–1690.

Gavezzotti, A. & Filippini, G. (1995). *J. Am. Chem. Soc.* **177**, 12299–12305.

Giese, B. & Meister, J. (1977). *Chem. Ber.* **110**, 2588–2600.

Grützmacher, H.-F. & Schmuck, R. (1980). *Chem. Ber.* **113**, 1192–1194.

Hillebrand, G. G. & Bisett, D. L. (1993). *J. Soc. Cosmet. Chem.* **44**, 129–138.

Hillebrand, G. G., Winslow, M. S., Heitmeyer, D. A. & Bisett, D. L. (1990). *J. Soc. Cosmet. Chem.* **41**, 187–195.

Johnson, J. E. & Jacobson, R. A. (1973). *Acta Cryst.* B**29**, 1669–1674.

Lagutkin, N. A., Mitin, N. I., Zubairov, M. M., Dorokhov, V. A. & Mikhailov, B. M. (1982). *Pharm. Chem. J.* pp. 464–467.

Mnyukh, Yu. V. (1979). *Mol. Cryst. Liq. Cryst.* **52**, 163–200.

Pyrka, G. J. & Pinkerton, A.A. (1992). *Acta Cryst.* C**48**, 91–94.

Richardson, M.R., Yang, Q.-C., Novotny-Bregger, E. & Dunitz, J. D. (1990). *Acta Cryst.* B**46**, 653–660.

Sheldrick, G. M. (1985). *SHELXS*86. *Program for the Solution of Crystal Structures.* University of Göttingen, Germany.

Sheldrick, G. M. (1990). *SHELXTL/PC User's Manual.* Siemens Analytical X-ray Instruments Inc., Madison, Wisconsin, USA.

Sheldrick, G. M (1993). *SHELXL*93. *Program for the Refinement of Crystal Structures.* University of Göttingen, Germany.

Siemens (1990). *XSCANS*2.10. Siemens Analytical X-ray Instruments Inc., Madison, Wisconsin, USA.

Tschitschibabin, A. E. & Zeide, O. A. (1914). *Zh. Russ. Khim. Ova.* **46**, 1216–1224.

Wibaut, J. P. & Dingemanse, E. (1923). *Recl Trav. Chim. Pays-Bas*, **42**, 240–250.